Long-Term and Accelerated Life Testing of a Novel Single-Wafer Vacuum Encapsulation for MEMS resonators

R. N. Candler[1], M. Hopcroft[1], B. Kim[1], W.-T. Park[1], R. Melamud[1], M. Agarwal[1], G. Yama[2], A. Partridge[3], M. Lutz[3], T. W. Kenny[1]
[1]Stanford University, Departments of Electrical and Mechanical Engineering
[2]Robert Bosch RTC
[3]Robert Bosch RTC, currently at SiTime

rcandler@stanford.edu, tel: 650-906-3356, fax: 650-723-3521

Abstract

We have developed a single wafer vacuum encapsulation for MEMS resonators, using a thick (20 μm) polysilicon encapsulation to package micromechanical resonators in a pressure < 1 Pa. The encapsulation is robust enough to withstand standard back-end processing steps, such as wafer dicing, die handling, and injection molding of plastic. We have continuously monitored the pressure of encapsulated resonators for more than 10,000 hours and have seen no measurable change of pressure inside the encapsulation at ambient temperature. We have subjected packaged resonators to > 600 cycles of –50-80°C and no measurable change in cavity pressure was seen. We have also performed accelerated leakage tests by driving hydrogen gas in and out of the encapsulation at elevated pressure. Two results have come from these hydrogen diffusion tests. First, hydrogen diffusion rates through the encapsulation at temperatures 300 – 400°C have been determined. Second, the package was shown to withstand multiple temperature cycles between room and 300 – 400°C without showing any adverse affects. The high robustness and stability of the encapsulation can be attributed to the clean, high temperature environment during the sealing process.

Introduction

Packaging and reliability remain a major hurdle for getting MEMS into commercial products, with the latter being heavily dependent on the former. Packaging is difficult, because handling and liquid processing can be very difficult for released MEMS structures. A known, stable environment is essential for reliable and repeatable performance over a long period of time, so that the MEMS device will be protected from potential behavior changing contaminants such as dust particles, moisture, gas molecules, etc.

The two primary methods for encapsulating MEMS devices at the wafer scale are use of a separately bonded cap or deposition of an encapsulation layer. There are multiple ways of bonding a cap onto a MEMS device, including anodic bonding of glass to silicon [1], and thermocompression bonding of glass to silicon [2] or silicon to silicon with a gold intermediate layer [2] [3]. The use of intermediate layers of solder, PSG [4], or glass frit [1, 5] to bond glass to silicon have been used to allow for more topology to be covered by the bond. Getters are sometimes used to control pressure inside the cavity and reduce the effect of any outgassing that occurs from the sealing material [5-7]. Several methods of bond formation via localized heating have been investigated. Advantages of localizing the heat to the bond area are better control of the bond temperature and the ability to attain a higher temperature at the bond as compared to the device, which mitigates concerns of thermal budget for circuitry or temperature sensitive materials. Localized heating with polysilicon [2, 4, 8, 9], and gold [2] microheaters for thermally activated bonding has been used, and a review of bonding via localized heating

from microheaters is given in [10]. Bonding via localized microwave heating is described in [11], while induction heating was used in [12].

Numerous encapsulation methods based on surface micromachining techniques also exist. Most involve the use of some sacrificial material to support deposition of an encapsulation layer, followed by removal of the sacrificial layer through some sort of etch access holes and then resealing of the etch holes. One method is the use of silicon dioxide as a sacrificial material, which is removed with liquid hydrofluoric acid (HF) after the deposition of the encapsulation (cap) layer, which has been silicon [13, 14], nitride [15-17], or metal deposited via electron beam deposition [18]. HF in the vapor phase has also been used with a low-temperature polysilicon seal for CMOS compatible packaging [19]. Another method uses a metal encapsulation, where the deposition method is electroplating and the sacrificial material is photoresist [20].

Other methods have also been used which avoid the use of a fluidic access port to remove the sacrificial material, preferring to remove the sacrificial through the encapsulation material. Thin layers of polysilicon, permeable to HF, were used in [21, 22]. Electrochemical etching was used to make the polysilicon encapsulation layer nanoporous, through which the sacrificial oxide was removed [23]. Low-cost options were also examined when polymeric materials were used as the sacrificial and encapsulating layer, with removal of the sacrificial layer occurring via thermal decomposition [24].

The importance of a stable pressure environment is not a new idea, as it has been studied in quartz resonators for many years [25]. Long-term and extreme environment studies of MEMS packaging has become more important as devices move toward

commercialization. Solder-sealed resonators were seen to have a decrease in Q over 1000 hours at 100°C due to outgassing of the solder [26]. Use of a getter was seen to stabilize Q [5]. A bonded silicon package for RF MEMS switches was tested at elevated temperature, pressure, and humidity, with test lifetimes of 100s of hours and projected ambient lifetimes of 100s of years [27]. Also, a bonded encapsulation of silicon resonators was seen to have no change in Q over 2 months at ambient conditions [28].

Our work uses selective deposition of epitaxial silicon and polysilicon to form a robust vacuum encapsulation over a sacrificial oxide layer. Previous work used a silicon encapsulation that was sealed with LPCVD oxide at 450°C [29-32]. Our current work seals the encapsulation during a silicon deposition step at temperatures > 900°C. Early results from this encapsulation process and testing have been reported in [33, 34], and included herein is extended data of > 1 year of testing and > 600 temperature cycles. The known gas environment and high temperature of the sealing process leads to a very stable vacuum environment for the encapsulated devices. In the following sections, a thorough study of the encapsulation hermiticity will be given. Long term (> 1 year) tests of resonators at room temperature, temperature cycling between -50°C and 80°C, and high temperature (300°C - 400°C) diffusion of hydrogen through the encapsulation will all be presented.

Fabrication

The "epi-seal" fabrication process begins with Deep Reactive Ion Etching (DRIE) of the resonator structure into the top silicon layer of an SOI wafer, Figure 1a. Next, the trenches of the unreleased resonator are sealed with a sacrificial layer of LPCVD oxide,

Figure 1b, and contact holes are etched into the oxide. These contacts provide electrical access to the encapsulated structures and mechanical support for the encapsulation layer. The silicon encapsulation layer is deposited in two steps. In the first step, a 2 μm "cap" layer of silicon is deposited on top of the sacrificial oxide and vent holes are etched through the cap layer to expose the oxide, Figure 1c. Vapor-phase hydrofluoric acid (HF) is then used to etch the sacrificial oxide and release the resonator structure. Use of HF in vapor phase has the advantage of avoiding stiction and making a critical point drying (CPD) process unnecessary. After etching the sacrificial oxide, the second part of the silicon encapsulation layer is deposited. This 20 μm thick "seal" layer closes the vent holes and provides mechanical stiffness, Figure 1d. Because it closes the vents, the seal deposition step defines the environment inside the encapsulated cavity when the process is complete. This epitaxial silicon deposition is performed at high temperature (950° C) in a low-pressure reactor with only hydrogen, silicon, and chlorine present, so the resulting environment inside the encapsulation is clean and stable. Also, single crystal silicon is deposited on existing single crystal silicon in this process, creating the possibility of integrating circuitry beside the resonator after the MEMS fabrication is complete (MEMS-first integration). Next, the wafer surface is planarized using chemical mechanical polishing (CMP) in order to eliminate the surface roughness of the thick epitaxial silicon and the topology over the encapsulated structures. At this point, the top surface of the wafer is indistinguishable from an ordinary blank silicon wafer. Ring-shaped trenches are now etched into the encapsulation layer, creating isolated pillars of silicon in the encapsulation for electrical feedthroughs, Figure 1e. Low Pressure Chemical Vapor Deposition (LPCVD) oxide is deposited to close the trenches, and

contact holes are etched into the oxide, Figure 1f. Finally, aluminum is deposited and patterned to make electrical connections and pads for applying signal to the resonator, Figure 1g.

Some features of the process are highlighted below. Views of the encapsulation after deposition, but before CMP planarization are given in Figure 2, which is the process step immediately after Figure 1d above.

Faceting between regions of polysilicon and single crystal silicon are shown in Figure 3. Silicon deposited on oxide is polycrystalline, while silicon deposited on single crystal silicon is single crystalline, leaving open the option for integration with circuitry after the MEMS processing. Location of vent holes that were etched into the silicon to allow HF vapor release of oxide (Figure 1c) and sealed (Figure 1e) are shown in Figure 4.

Testing

Two testing methods were used for these resonators, custom circuit board and wafer probe station. The custom circuit boards were used for the long term testing and the -50°to 80°C thermal cycling, while the wafer probe station was used for the 300 °C - 400 °C hydrogen diffusion tests. The long term and thermal cycling tests were performed

with resonators mounted on custom circuit boards in a temperature-controlled chamber Figure 5.

Two resonator designs, designated “design A” and “design B” were used for the long-term testing, Figure 6 and Figure 7. Design A is a pair of single-anchored double-ended tuning fork structures. That is, each tuning fork structure has couplings between the beams (6 μm thick) at both ends, but the structure is only anchored to the substrate at one end. Two of these tuning forks are used for the device and are coupled at the anchor in an effort to build a symmetric structure that minimizes energy loss through the anchor. Design B is also a pair of single-anchored double-ended tuning forks, except that design B has a mass at the end of the tuning forks that is not anchored (beam thickness = 8 μm). Both design A and design B were in a regime where Q was limited to pressure. To determine this, the encapsulation was removed from the parts, which were then placed in a vacuum chamber. The Q in the vacuum chamber was higher than the encapsulated pressure, indicating that the encapsulated parts have air-damping limited Q. This is critical, as the Q of the resonators is used to determine if the cavity pressure is changing.

Long-term testing

Three resonators of design A and two of design B were tested at constant temperature 25°C ± 0.1°C over many months. As can be seen in Figure 8, the quality

factor, Q, is stable over > 10,000 hours. Voids in the data are caused by test setup maintenance or power outages, and offset steps in the temperature signal are due to a fluctuating ground level in the temperature sensing circuit.

Since the Q of these devices is limited by pressure, any change in cavity pressure would result in a corresponding change in Q. The pressure can be inferred from Q via a calibration. The encapsulation was intentionally removed from three design A resonators, and the resonators were measured at several pressures in a vacuum chamber, Figure 9. By equating the Q of an encapsulated resonator with the Q in the Q vs. pressure curve of Figure 9, the pressure inside the encapsulation can be inferred. A design B resonator, encapsulation removed, was also tested at low pressure to confirm that the part was limited by air damping and acting as an effective pressure sensor, although a full Q .vs pressure curve was only collected for design A.

There is one subtle point that should be made regarding the actual gas pressure inside the cavity. The vacuum chamber measurement was performed with air as the ambient gas, while the ambient of encapsulated resonators is almost exclusively hydrogen, as mentioned in the fabrication section. Because of this, the pressure value given by matching the Q of encapsulated and vacuum chamber devices is the *air pressure* that provides equivalent damping as the gas in the cavity. However, the gas inside the cavity is primarily hydrogen. Since hydrogen has less mass than the average gas molecule in air, the *hydrogen pressure* that provides the same damping (and therefore the same Q) as air will be higher. Using a simple air damping equation, Q can be seen to

scale as $Q \propto \frac{1}{\sqrt{m}}$ [35], where m is the molecular mass of the gas. From this, the hydrogen pressure that provides equivalent damping as air would be ~4 times greater than the air pressure. Thus, it is possible to find the actual hydrogen pressure inside the cavity. However, referring the damping to equivalent air pressure is an easier way to standardize the pressure damping, since most pressure-damped resonators are measured in air. All of the subsequent pressures are equivalent air pressures, unless otherwise specified.

The Q vs. pressure relationship from Figure 9 can be used to convert Q to equivalent air pressure in Figure 10. The result of these tests is that no measurable change in pressure could be seen over 1 year of measurement. The next step is to generate harsher conditions by subjecting the package to a range of temperatures.

Temperature cycles

Resonators were subjected to thermal cycling in order to further test package robustness. Two design A resonators, mounted on circuit boards, were placed in a thermal chamber, and Q was measured at 30°C. The oven temperature was increased to 80°C, decreased to 30°C, stabilized, and the resonator Q was measured again. The oven temperature was decreased to -50°C, increased to 30°C, and the resonator Q was again measured. This cycle was repeated > 600 times, and no decrease in Q could be seen, Figure 11. If anything, a very slight increase in Q was observed. This is evidence that the

package is robust and can withstand these temperature changes without compromise of the package integrity. It also demonstrates that there is no significant outgassing from the package at these temperatures. The lack of outgassing is a reasonable expectation, as the final package seal was performed at 950°C . Also, there is no observable hysteresis between measurements after an 80°C ramp and -50°C ramp. Since there was no strong effect seen in this experiment, more extreme temperatures of up to 400°C were used to measure diffusion through the encapsulation, which is discussed in the next section. Even at this higher temperature not all gasses were seen to diffuse through the encapsulation, as hydrogen diffusion was observed and nitrogen diffusion was not.

Accelerated Testing

Since no pressure decrease was observed in either the long-term measurements at room temperature or the thermal cycle tests from -50°C to 80°C, more extreme conditions were used to measure diffusion of gasses through cavity. These conditions involved changing both the temperature and gas composition of the ambient. Packaged resonators, designated as "design C" resonators were used for this study. Design C resonators are doubly-clamped tuning forks with beam length = 540 μm and beam thickness = 8 μm. The higher frequency of design C resonators over design A and B was preferable, because a higher pressure could be measured before the Q dropped so low that the devices could not be measured. The resonators were placed in a 400°C furnace with a hydrogen environment (hydrogen: nitrogen = 1:5 at atmospheric pressure) for 1 hour. After this furnace treatment, the Q of the resonators dropped to below 200, indicating that

an extreme pressure damped condition had been created. As is shown below, Figure 13, this pressure damped condition could be undone with furnace treatments with nitrogen ambient, suggesting that hydrogen could diffuse through the encapsulation at this temperature, while nitrogen could not. Thus, placing the packaged resonators that have hydrogen in the encapsulation into a furnace with nitrogen-only ambient would generate a partial pressure gradient that would act to pull the hydrogen out of the encapsulation. Since the ambient gas, nitrogen, can not diffuse into the encapsulation because of its larger size, the overall pressure in the encapsulation decreases.

As was done in the previous experiments, a relationship between Q and pressure was obtained by measuring a resonator, encapsulation removed, inside a vacuum chamber. The result of this measurement is shown in Figure 14, and an equation, derived from the experimental data, relating Q and pressure (valid for pressures > 20 Pa) is given by equation 1. Only data for pressures > 20 Pa was used, because the Q vs. pressure curve levels out at lower pressures, amplifying any uncertainty in Q to a much greater uncertainty in pressure.

$$Q = \frac{123000}{P^{0.98155}} \tag{1}$$

Using the data from Figure 13 and Figure 14, a relationship between anneal time and pressure can be obtained. The pressure vs. time should follow the diffusion relationship of equation 2, where P(t) is the encapsulation pressure, P_0 is the initial encapsulation

pressure, $P_{ambient}$ is the pressure outside the encapsulation, and D is a diffusion coefficient that is temperature dependent.

$$P(t) = P_{ambient} + (P_0 - P_{ambient})e^{-Dt} \tag{2}$$

Assuming that the hydrogen pressure is negligible during the nitrogen furnace treatments, equation 2 reduces to equation 3.

$$P(t) = P_0 e^{-Dt} \tag{3}$$

The experimental data follows the trend predicted by equation 3, Figure 15, and the diffusion coefficient can be extracted for the furnace treatments at 400°C. Hydrogen was diffused back into the encapsulation via a 400°C hydrogen furnace treatment, and the removal of hydrogen was repeated for 350°C and 300°C, also shown in Figure 15.

The diffusion coefficient, D, was extracted for each of the three temperatures investigated. An Arrhenius equation was extracted from the diffusion coefficients, shown in equation 4.

$$D = 60e^{-\frac{3529}{T}} \tag{4}$$

The diffusion coefficients extracted from Figure 15, along with equation 4, are shown in Figure 16. The extrapolation of the equation to lower temperatures shows that the simple

extrapolation overestimates the diffusion coefficient as compared to experimental data at room temperature. The diffusion coefficient extracted from room temperature is an absolute worst-case value. As was mentioned before, there was no measurable drop in pressure for packaged resonators at room temperature over one year. In order to get an upper limit on room temperature diffusion coefficient, a trend line was drawn through the long-term data that did not average out the measurement noise. Thus, the upper limit on room temperature diffusion is very likely overestimated, due to the noise in the measurement. The difference between the diffusion coefficient at room temperature and the diffusion coefficient extrapolated to room temperature from higher temperatures is not unexpected, as the diffusion process of hydrogen through these materials is a complex process [36].

It is important to note that the diffusion constant is species specific. Hydrogen, being the smallest element, is likely to have one of the largest diffusion coefficients. While the hydrogen time constant, $\tau = \frac{1}{D}$, may be as small as thousands of hours, there are three mitigating factors that suggest very long term hermiticity of the encapsulation. (1) Long term experimental results from the previous section bound the diffusion time constant at room temperature to greater than 50,000 hours. The limiting factor from these long term experiments is thought to be from measurement noise, and not from actual diffusion of gas into the encapsulation. The difference between the room temperature time constant extrapolated from high temperature data and the time constant measured at room temperature are, as stated above, an indication of the complex dependence of

diffusion on temperature. That is, it is possible that the diffusion coefficient falls off very rapidly as temperature decreases, and our estimates and measurements are overly conservative by an order of magnitude or more. (2) Other species that might diffuse in will be larger and are likely to diffuse more slowly. A piece of supporting evidence comes from the nitrogen furnace steps that were used to diffuse hydrogen out of the encapsulation. If the nitrogen could diffuse in at a rate comparable to the rate at which hydrogen diffuses out, the Q would not increase over time. If the nitrogen could diffuse at a rate slower than the hydrogen but in the same order of magnitude, the pressure would decrease, then increase. This would signify that hydrogen leaves the encapsulation, and then nitrogen diffuses in gradually. However, neither of these behaviors was observed, indicating that the rate of nitrogen diffusion through the encapsulation is *much slower* than the rate of hydrogen diffusion. This leads to the third factor. (3) There is a very small percentage of hydrogen in the atmosphere. Hydrogen only makes up 0.00005% of the atmosphere [37], so even if the inside of the encapsulation were equilibrated with the partial pressure of atmospheric hydrogen, the pressure inside the cavity would still be very low. Helium, the next smallest element, is also a low fraction of the atmosphere, 0.0005%. The most abundant element, nitrogen at 78.08%, was determined to diffuse very slowly through the encapsulation, as evidenced by its lack of an effect on encapsulation pressure from high temperature nitrogen furnace processes.

Conclusions

A single-wafer encapsulation for micromechanical resonators was presented. Long-term hermiticity of the encapsulation was demonstrated with > 1 year of Q (and

thereby pressure) monitoring. Temperature cycles between -50°C and 80°C were performed > 600 times, and no degradation of Q was seen. Finally, hydrogen was diffused in and out of the cavity at different temperatures between 300°C and 400°C, giving quantitative information of diffusion of hydrogen out of the cavity at higher temperatures, as well as demonstrating the extreme robustness of the packaging method. The encapsulation technique is suitable for several other types of sensors (*e.g.* inertial sensors) in addition to resonators, and the silicon deposition process leaves open the option of MEMS-last integration.

Acknowledgements

This work was supported by DARPA HERMIT (ONR N66001-03-1-8942), Bosch Palo Alto Research and Technology Center, a CIS Seed Grant, The National Nanofabrication Users Network facilities funded by the National Science Foundation under award ECS-9731294, and The National Science Foundation Instrumentation for Materials Research Program (DMR 9504099).

References

[1] M. Lutz, W. Golderer, J. Gerstenmeier, J. Marek, B. Maihofer, S. Mahler, H. Munzel, and U. Bischof, "A precision yaw rate sensor in silicon micromachining," *International Conference on Solid State Sensors and Actuators, TRANSDUCERS '97*, vol. 2, pp. 847-850 vol.2, 1997.

[2] Y. T. Cheng, L. Lin, and K. Najafi, "Localized silicon fusion and eutectic bonding for MEMS fabrication and packaging," *Journal of Microelectromechanical Systems*, vol. 9, pp. 3-8, 2000.

[3] C. H. Tsau, S. M. Spearing, and M. A. Schmidt, "Fabrication of Wafer-Level Thermocompression Bonds," *Journal of Microelectromechanical Systems*, vol. 11, pp. 641-647, 2002.

[4] Y. T. Cheng, L. Lin, and K. Najafi, "Localized bonding with PSG or indium solder as intermediate layer," *Twelfth IEEE International Conference on Micro Electro Mechanical Systems*, pp. 285-289, 1999.

[5] D. Sparks, S. Massoud-Ansari, and N. Najafi, "Long-term evaluation of hermetically glass frit sealed silicon to Pyrex wafers with feedthroughs," *Journal of Micromechanics and Microengineering*, pp. 1560-1564, 2005.

[6] Y. Jin, Z. Wang, L. Zhao, P. C. Lim, J. Wei, and C. K. Wong, "Zr/V/Fe thick film for vacuum packaging of MEMS," *Journal of Micromechanics and Microengineering*, pp. 687-692, 2004.

[7] D. Sparks, S. Massoud-Ansari, and N. Najafi, "Chip-Level Vacuum Packaging of Micromachines Using NanoGetters," *IEEE Transactions on Advanced Packaging*, vol. 26, pp. 277-282, 2003.

[8] Y.-T. L. Cheng, L.; Najafi, K., "A hermetic glass-silicon package formed using localized aluminum/silicon-glass bonding," *Journal of Microelectromechanical Systems*, vol. 10, pp. 392-399, 2001.

[9] Y.-T. Cheng, W.-T. Hsu, K. Najafi, C. T.-C. Nguyen, and L. Lin, "Vacuum packaging technology using localized aluminum/silicon-to-glass bonding," *Journal of Microelectromechanical Systems*, vol. 11, pp. 556-565, 2002.

[10] L. Lin, "MEMS post-packaging by localized heating and bonding," *IEEE Transactions on Advanced Packaging*, vol. 23, pp. 608-616, 2000.

[11] N. K. Budraa, H. W. Jackson, M. Barmatz, W. T. Pike, and J. D. Mai, "Low pressure and low temperature hermetic wafer bonding using microwave heating," *Micro Electro Mechanical Systems, 1999. MEMS '99. Twelfth IEEE International Conference on*, pp. 490-492, 1999.

[12] H.-A. Yang, M. Wu, and W. Fang, "Localized induction heating solder bonding for wafer level MEMS packaging," *Journal of Micromechanics and Microengineering*, pp. 394-399, 2005.

[13] K. Ikeda, H. Kuwayama, T. Kobayashi, T. Watanabe, T. Nishikawa, T. Yoshida, and K. Harada, "Three-Dimensional Micromachining of Silicon Pressure Sensor Integrating Resonant Strain Gauge on Diaphragm," *Sensors and Actuators A*, vol. A21-A23, pp. 1007-1010, 1990.

[14] J. D. Zook, W. Herb, A. Yongchul, and H. Guckel, "Polysilicon sealed vacuum cavities for microelectromechanical systems," *J. Vac. Sci. Tehcnol. A*, pp. 2286-2294, 1999.

[15] C. M. Mastrangelo and R. S. Muller, "Vacuum-sealed silicon micromachined incandescent light source," *Proceedings of the International Electron Devices Meeting*, pp. 503-506, 1989.

[16] C. H. Mastrangelo, J. H.-J. Yeh, and R. S. Muller, "Electrical and optical characteristics of vacuum-sealed polysilicon microlamps," *IEEE Transactions on Electron Devices*, vol. 39, pp. 1363-1375, 1992.

[17] L. H. Lin, R.T.; Pisano, A.P., "Microelectromechanical filters for signal processing," *Journal of Microelectromechanical Systems*, vol. 7, pp. 286-294, 1998.

[18] M. Bartek, J. A. Foerster, and R. F. Wolfenbuttel, "Vacuum sealing of microvacities using metal evaporation," *Sensors and Actuators A*, vol. 61, pp. 364-368, 1997.

[19] R. Aigner, K.-G. Opperman, H. Kapels, and S. Kolb, ""Cavity Micromachining" Technology: Zero-Package Solution for Inertial Sensors," *Transducers '01*, pp. 186-189, 2001.
[20] B. H. Stark and K. Najafi, "A Low-Temperature Thin-Film Electroplated Metal Vacuum Package," *Journal of Microelectromechanical Systems*, vol. 13, pp. 147-157, 2004.
[21] K. S. Lebouitz, A. Mazaheri, R. T. Howe, and A. P. Pisano, "Vacuum encapsulation of resonant devices using permeable polysilicon," *Twelfth IEEE International Conference on Micro Electro Mechanical Systems. MEMS '99*, pp. 470-475, 1999.
[22] T. Tsuchiya, Y. Kageyama, H. Funabashi, and J. Sakata, "Polysilicon vibrating gyroscope vacuum-encapsulated in an on-chip micro chamber," *Sensors and Actuators A*, vol. 90, pp. 49-55, 2001.
[23] R. He and C. J. Kim, "On-Chip Hermetic Packaging Enabled by Post-Deposition Electrochemical Etching of Polysilicon," *International Conference on Microelectromechanical Systems (MEMS 2005)*, pp. 544-547, 2005.
[24] P. Monajemi, P. J. Joseph, P. A. Kohl, and F. Ayazi, "A Low Cost Wafer-Leve MEMS Packaging Technology," *International Conference on Microelectromechanical Systems (MEMS 2005)*, pp. 634-637, 2005.
[25] D. E. Pierce, R. A. Murray, R. Lareau, S. Laffey, and J. R. Vig, "Outgassing of Quartz," *IEEE International Frequency Control Symposium*, pp. 107-114, 1994.
[26] D. Sparks, G. Queen, R. Weston, G. Woodward, M. Putty, L. Jordan, S. Zarabadi, and K. Jayakar, "Wafer-to-Wafer bonding of nonplanarized MEMS surfaces using solder," *Journal of Micromechanics and Microengineering*, pp. 630-634, 2001.
[27] A. Margomenos and L. P. B. Katehi, "Fabrication and accelerated hermiticity testing of an on-wafer package for RF MEMS," *Journal of Microelectromechanical Systems*, vol. 52, pp. 1626-1636, 2004.
[28] V. Kaajakari, J. Kiihamaki, A. Oja, H. Seppa, S. Pietikainen, V. Kokkala, and H. Kuisma, "Stability of Wafer Level Vacuum Encapsulated Single-Crystal Silicon Resonators," presented at Transducers 2005, 2005.
[29] A. Partridge, "Lateral Piezoresistive Accelerometer with Epipoly Encapsulation," in *Electrical Engineering*: Stanford University, 2003.
[30] R. N. Candler, W.-T. Park, H. Li, G. Yama, A. Partridge, M. Lutz, and T. W. Kenny, "Single Wafer Encapsulation of MEMS Devices," *IEEE Transactions on Advanced Packaging*, vol. 26, pp. 227-232, 2003.
[31] A. Partridge, A. E. Rice, T. W. Kenny, and M. Lutz, "New thin film epitaxial polysilicon encapsulation for piezoresistive accelerometers," *14th IEEE International Conference on Micro Electro Mechanical Systems, MEMS 2001*, pp. 54-59, 2001.
[32] W.-T. Park, R. N. Candler, S. Kronmueller, M. Lutz, A. Partridge, G. Yama, and T. W. Kenny, "Wafer-Scale Film Encapsulation of Micromachined Accelerometers," *Transducers '03*, vol. 2, pp. 1903 - 1906, 2003.
[33] R. N. Candler, W.-T. Park, M. Hopcroft, B. Kim, and T. W. Kenny, "Hydrogen Diffusion and Pressure Control of Encapsulated MEMS Resonators," *Transducers '05*, pp. 920-923, 2005.

[34] B. Kim, R. N. Candler, M. Hopcroft, M. Agarwal, W.-T. Park, J. Li, and T. W. Kenny, "Investigation of MEMS Resonator Characteristics During Long-Term and Wide Temperature Variation Operation," *2004 ASME International Mechanical Engineering Congress and RD&D Expo*, 2004.
[35] W. E. Newell, "Miniaturization of Tuning Forks," *Science*, pp. 1320-1326, 1968.
[36] N. H. Nickel, "Hydrogen Diffusion Through Silicon/Silicon Dioxide Interfaces," *J. Vac. Sci. Tehcnol. B*, vol. 18, pp. 1770-1772, 2000.
[37] R. G. Barry and R. J. Chorley, *Atmosphere, Weather and Climate*, 1998.

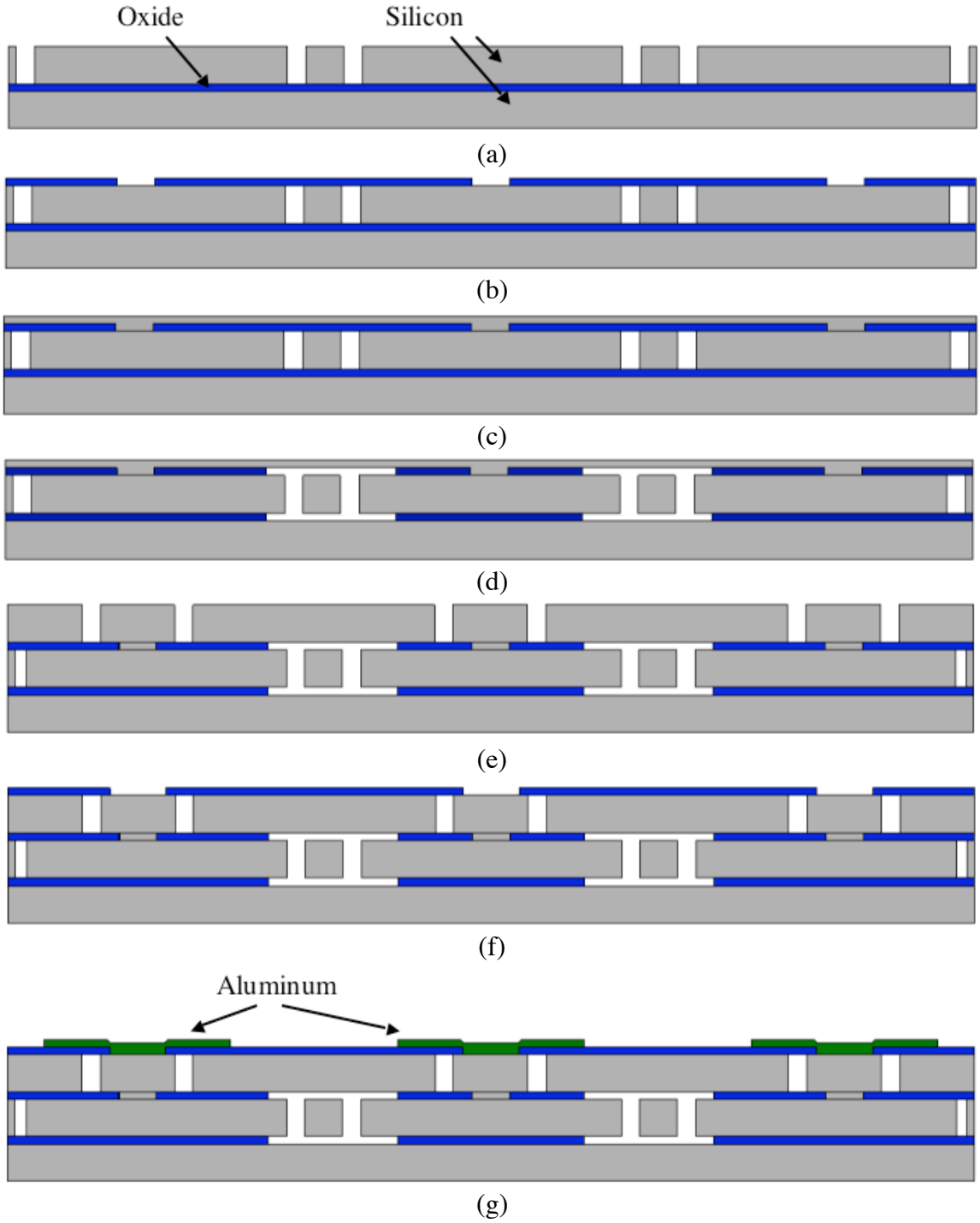

Figure 1. Fabrication process cross-section drawing. (a) resonator structure defined in top layer of SOI (b) resonator trenches resealed with oxide and etched to allow electrical contact to structure (c) 2 µm layer of silicon deposited and vent holes etched to allow HF vapor access for release of resonant beams (d) HF vapor process used to release resonator (e) resonators sealed in encapsulation with silicon deposition at 950°C, followed by CMP planarization and etching of cap layer to define electrical

contacts through cap (f) oxide deposited to seal over trenches and etched to allow electrical contact (g) aluminum deposited and etched for final contact.

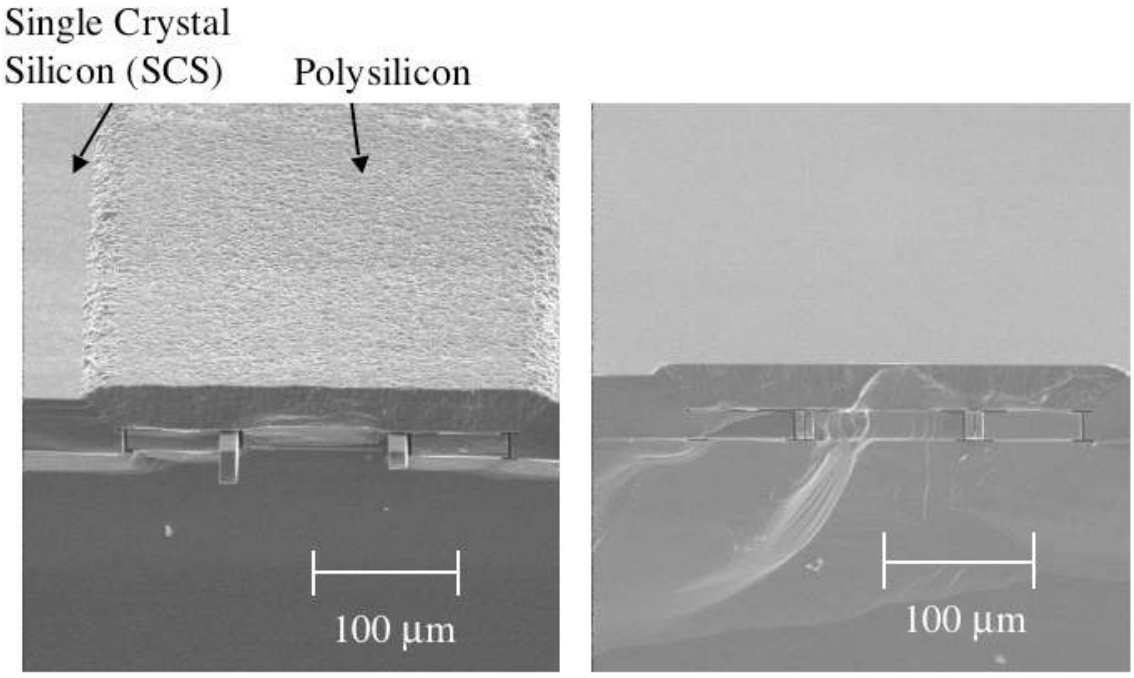

Figure 2. SEM cross-section after deposition of encapsulation, before CMP. The step height between polysilicon and single crystal silicon, caused by an oxide step and different deposition rates for single and polycrystalline silicon, can be seen on the right. This step height, along with the roughness of the polysilicon, necessitates CMP.

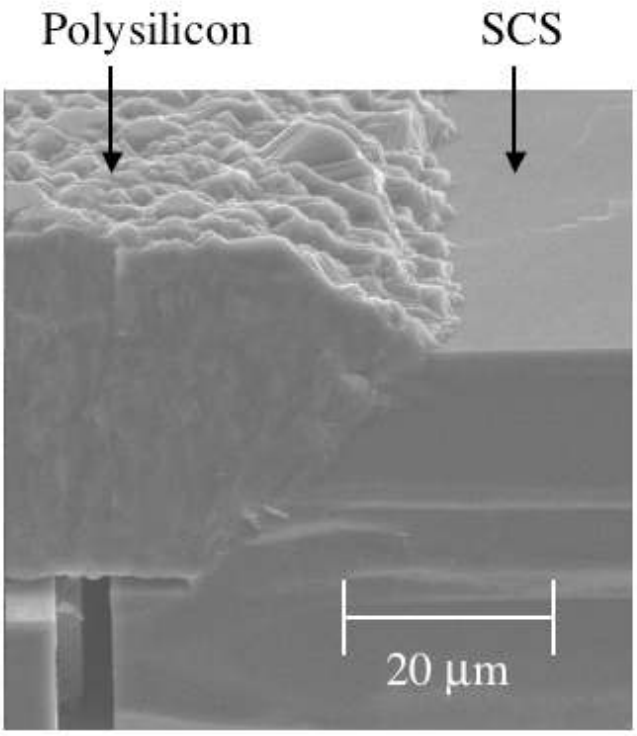

Figure 3. SEM of faceting between polysilicon and single crystal silicon (SCS).

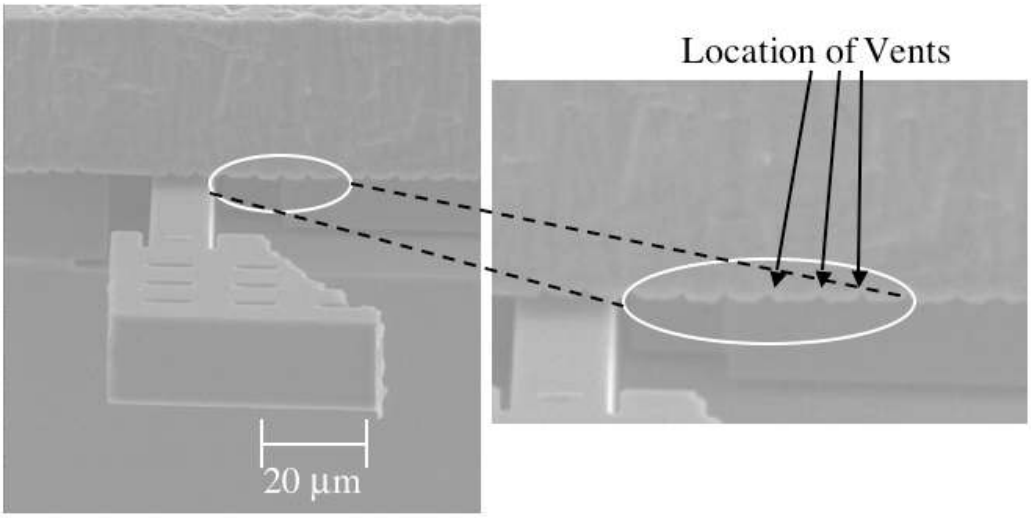

Figure 4. SEM of resealed vent holes, which were etched in Figure 1c, which are resealed in Figure 1e.

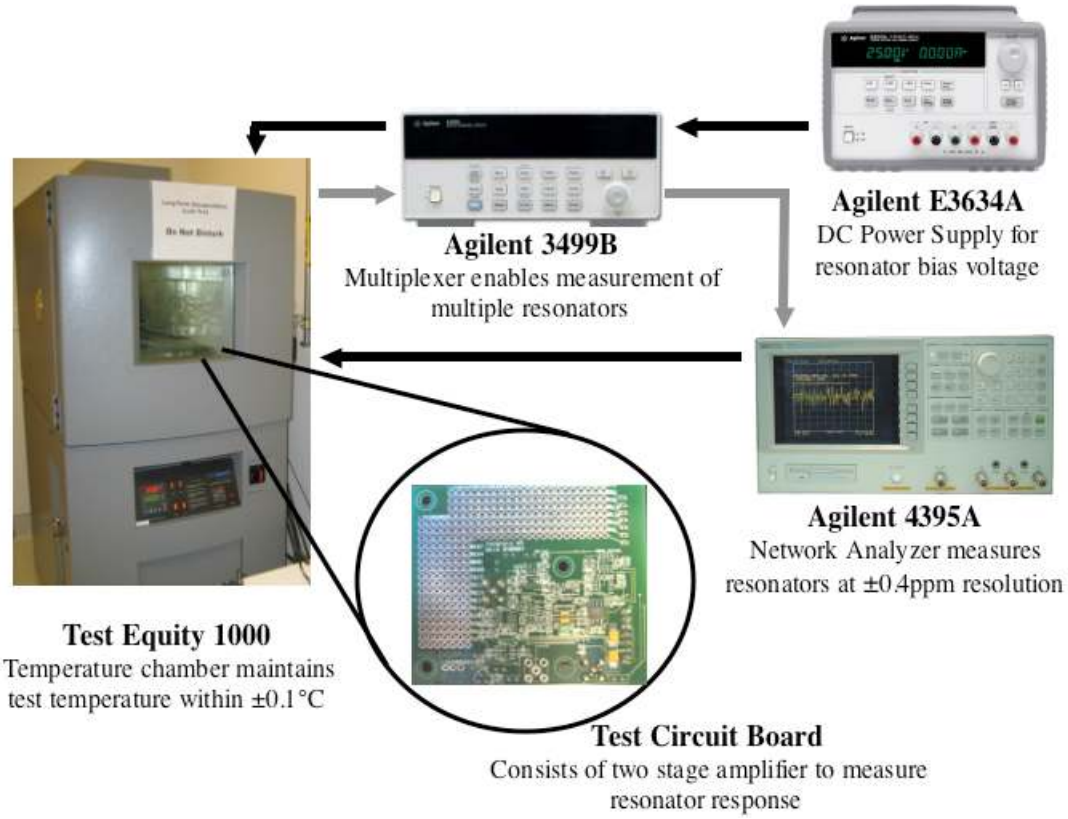

Figure 5. Schematic of test setup for multiple resonators in temperature chamber for long term testing. Resonator response, temperature, and bias voltage are multiplexed for reading of multiple resonators.

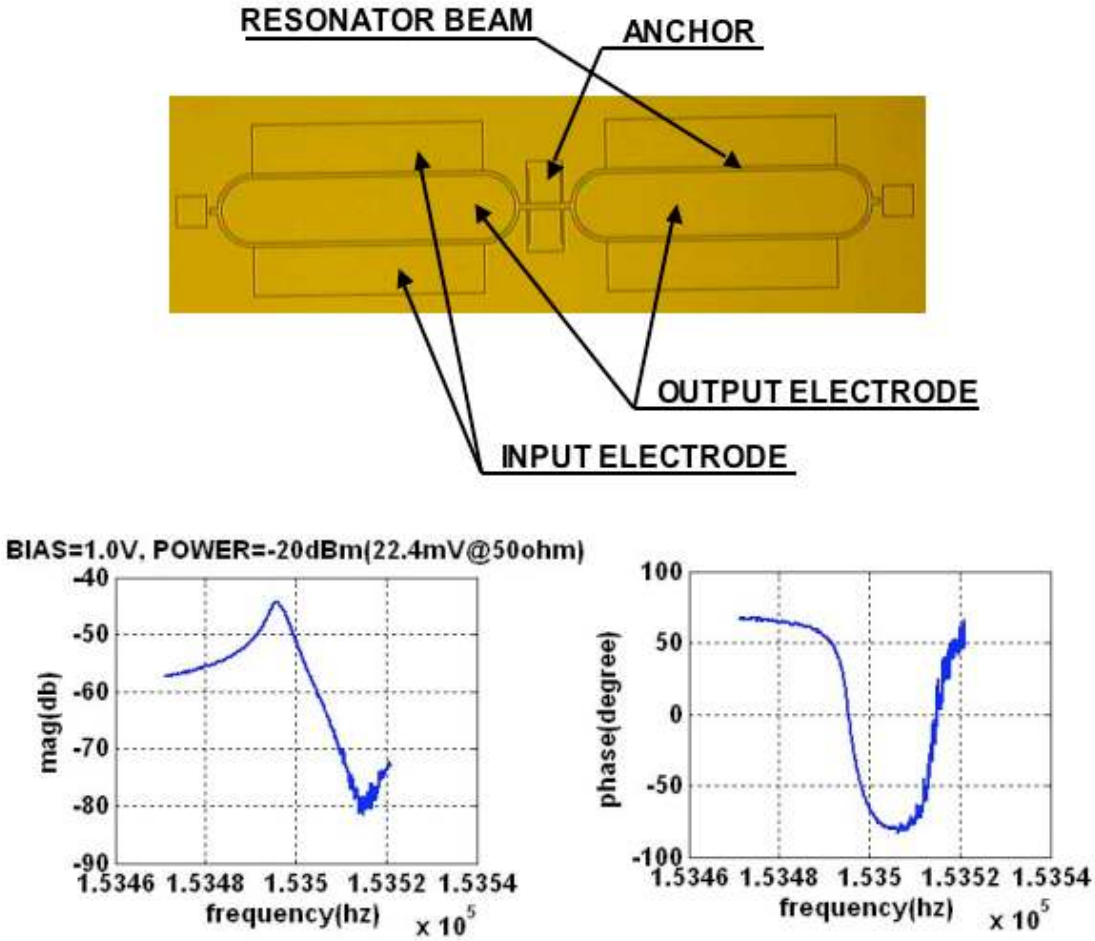

Figure 6. "Design A" resonator. Resonant frequency ≈ 150 kHz, Q ≈ 33,000.

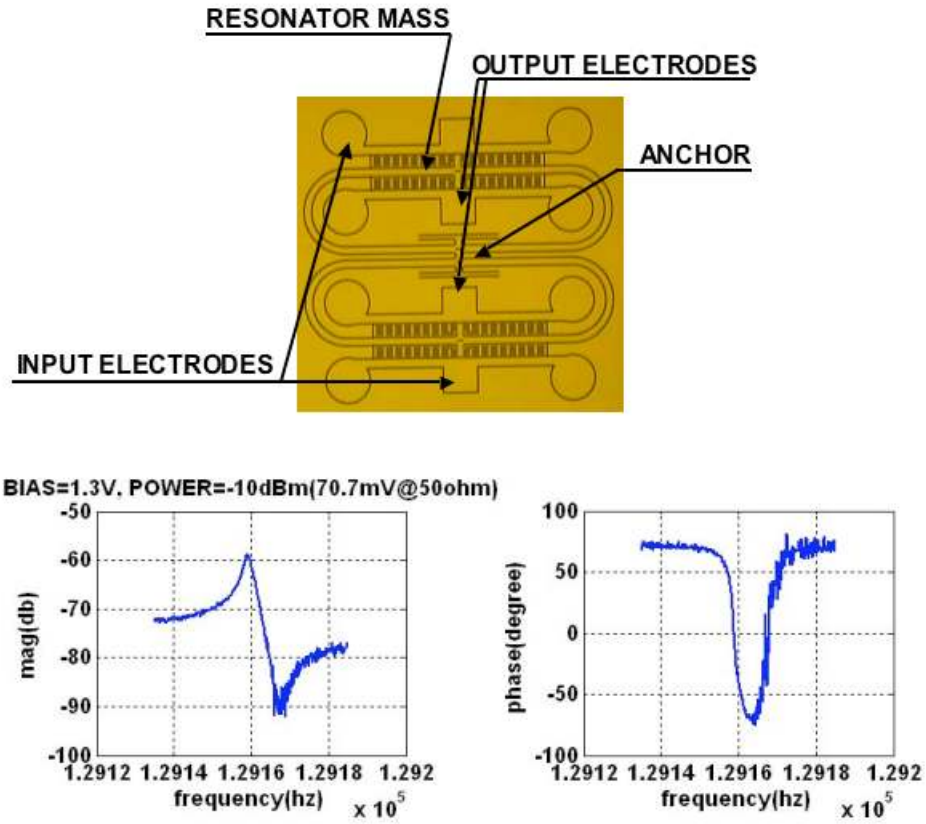

Figure 7. "Design B" resonator. Resonant frequency ≈ 130 kHz, Q ≈ 50,000.

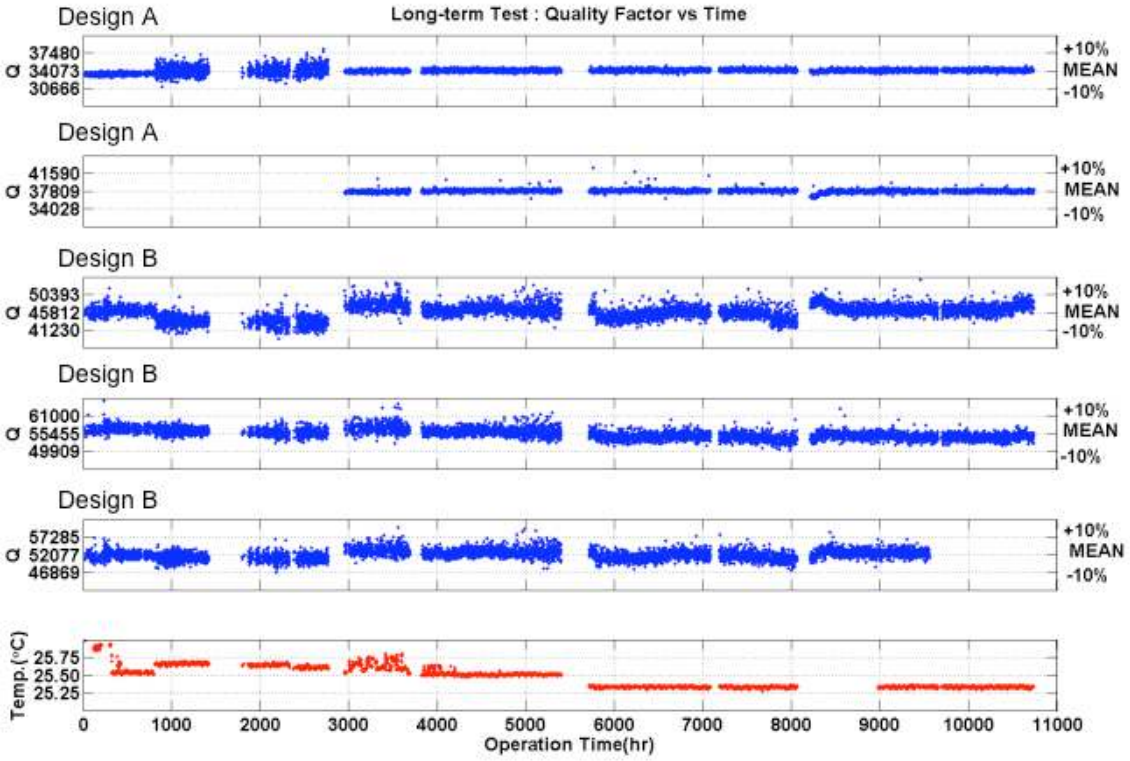

Figure 8. Long term test data for resonators under constant temperature (25°C ± 0.1°C).

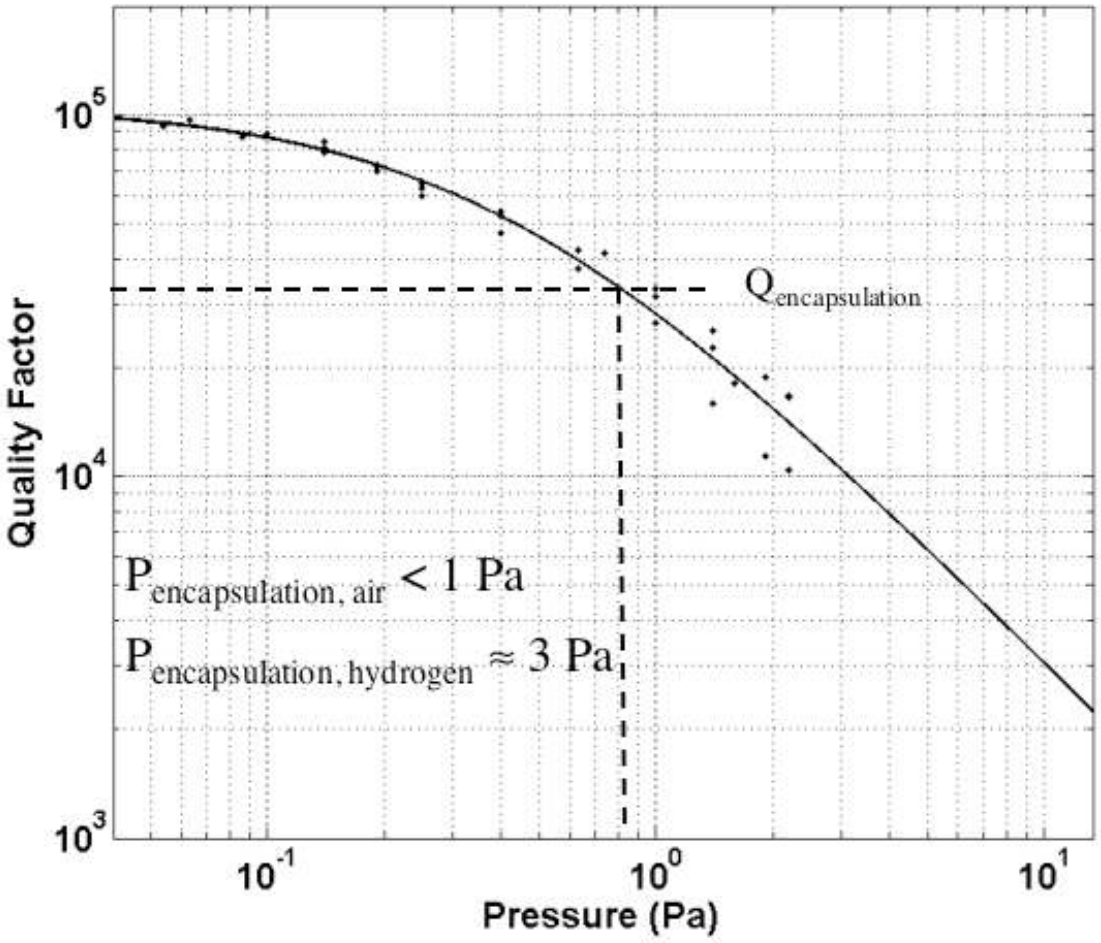

Figure 9. Q vs. pressure calibration curve for three design A resonators. Q of encapsulated device can be used to determine encapsulation pressure (both equivalent encapsulation pressure for air in cavity and scaled pressure for hydrogen in cavity).

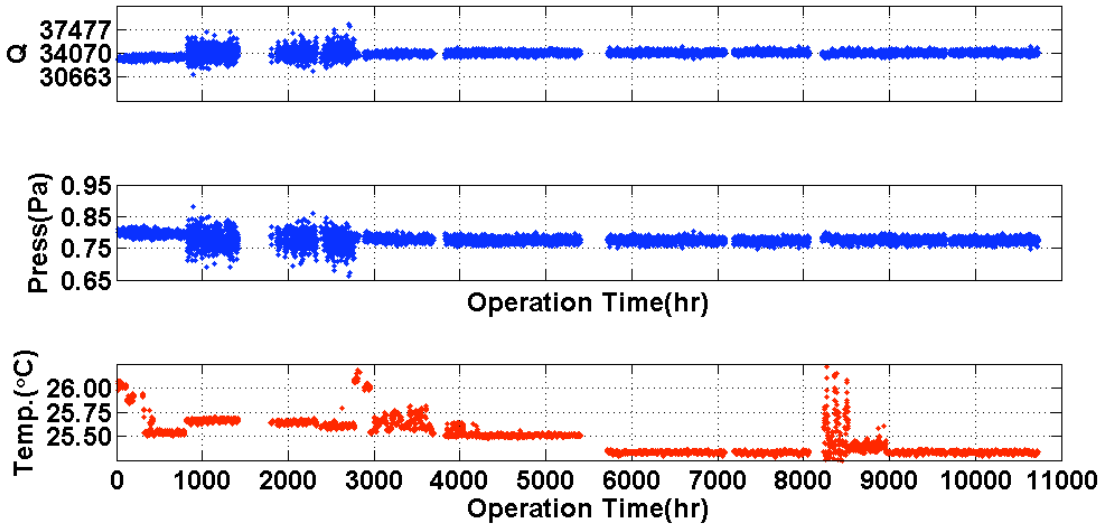

Figure 10. Pressure vs. time for Design A resonator.

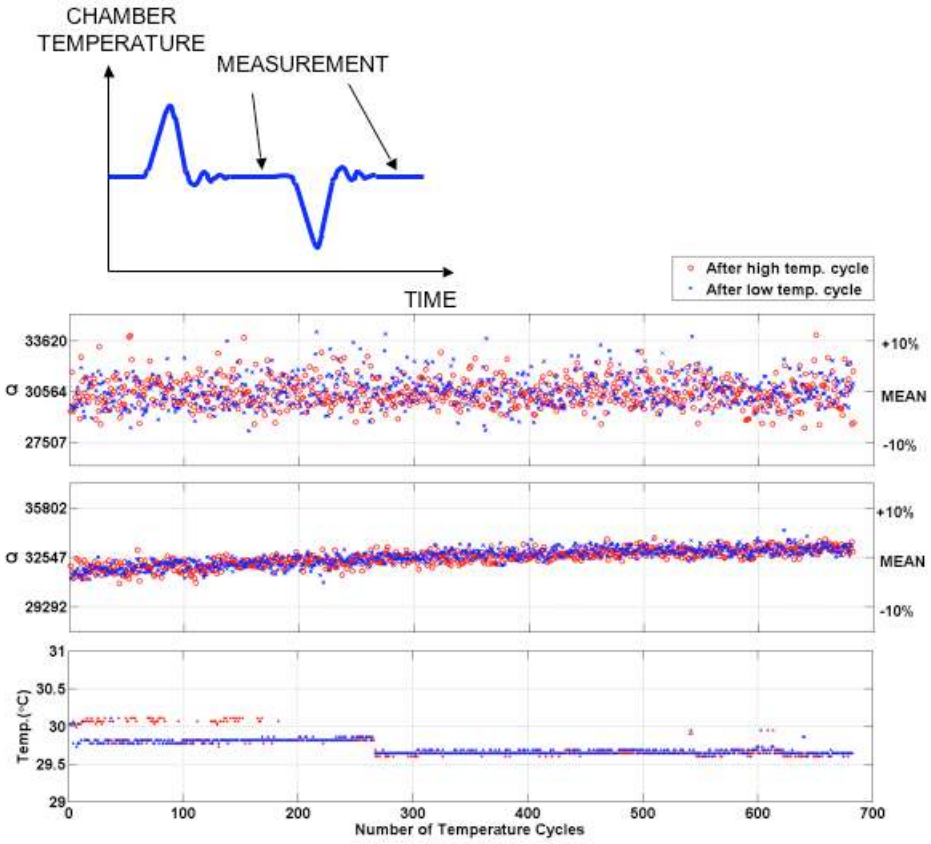

Figure 11. Q of two design A resonators at room temperature between cycles to 80°C and -50°C

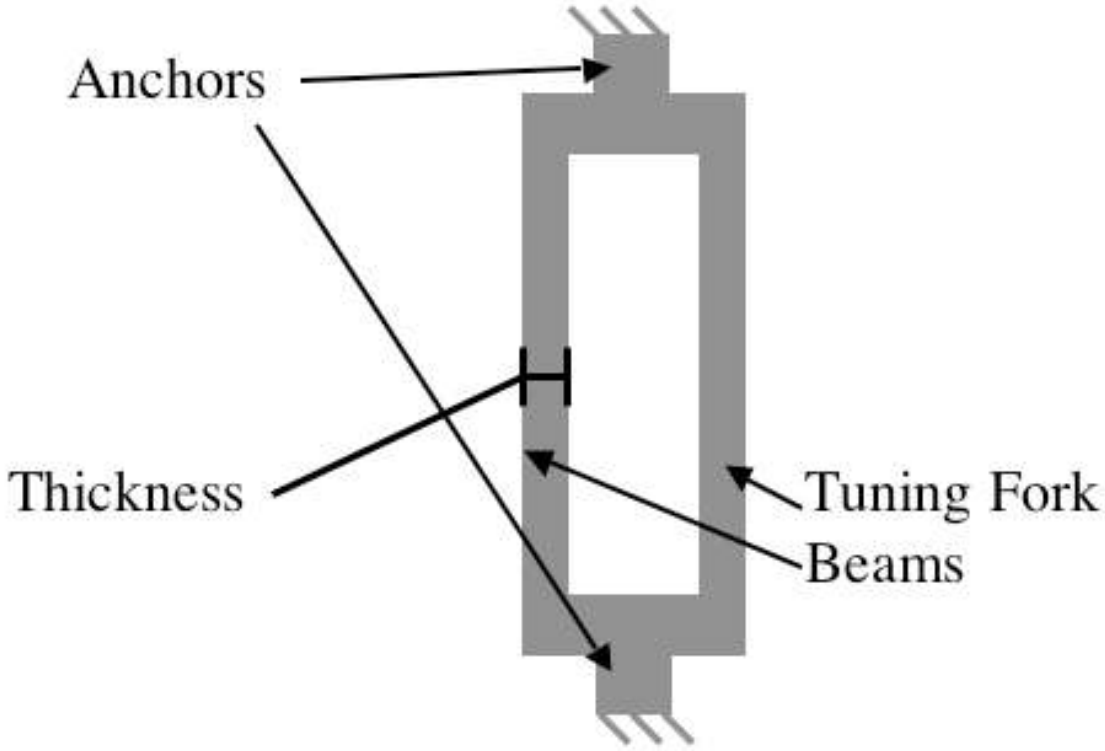

Figure 12. “Design C” resonators, resonant frequency ≈ 297 kHz.

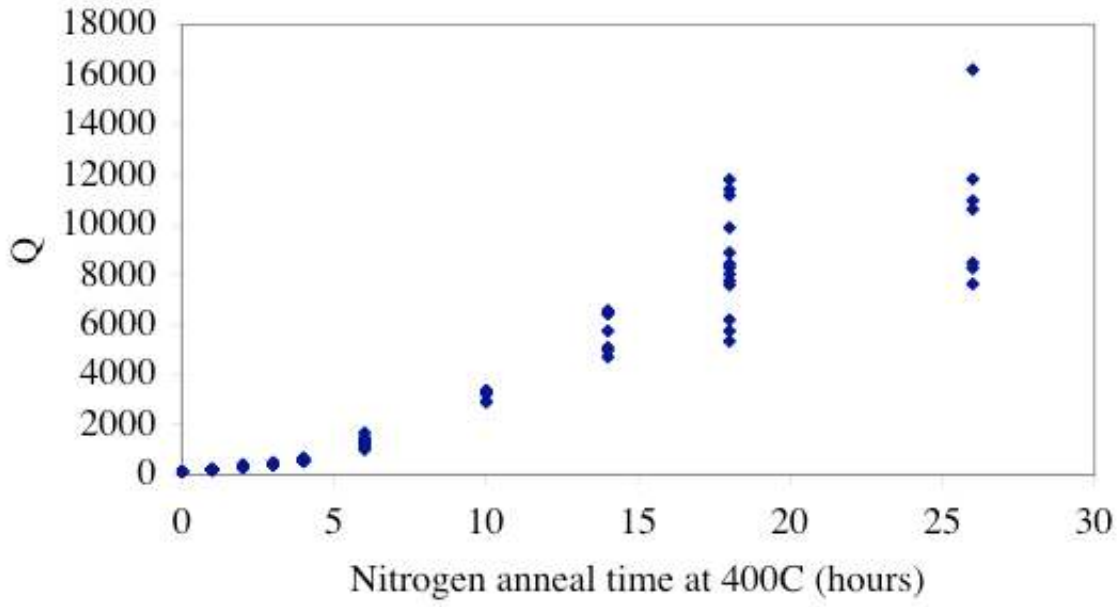

Figure 13. Removal of hydrogen from encapsulated resonators. Hydrogen was forced into the cavity with a hydrogen furnace treatment at 400°C. The hydrogen was removed with a series of nitrogen furnace treatments. As is seen in this data, the Q increased during these nitrogen furnace treatments, because the pressure inside the cavity was decreasing. At least 7 different design C resonators were measured after each furnace treatment.

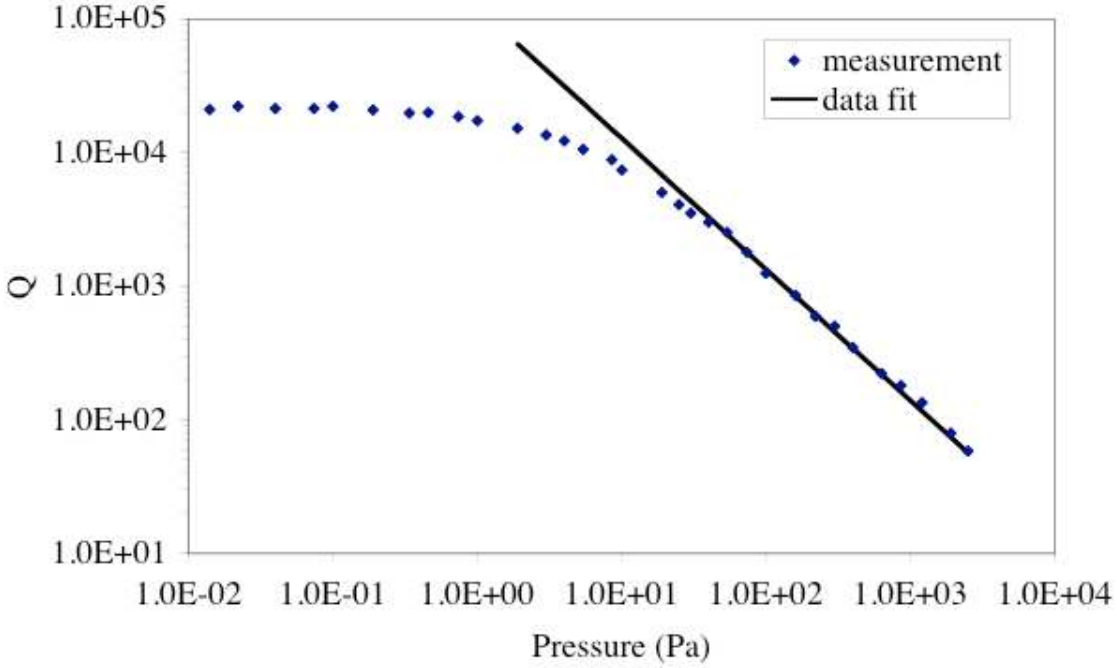

Figure 14. Q vs. pressure for design C resonator used in accelerated diffusion tests.

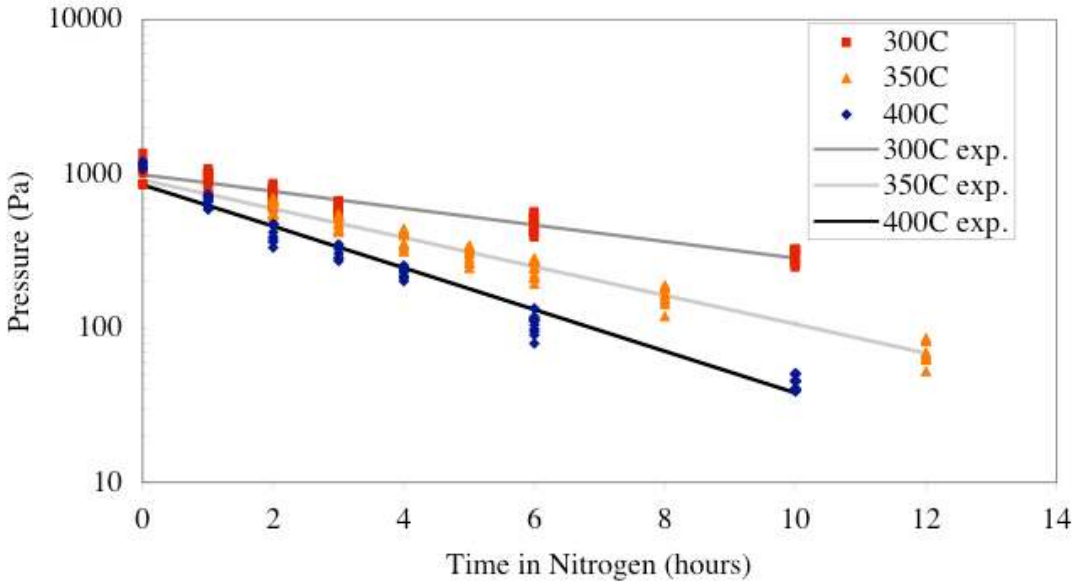

Figure 15. Pressure vs. time in nitrogen for different temperatures. As can be seen, exponential decay of pressure is followed.

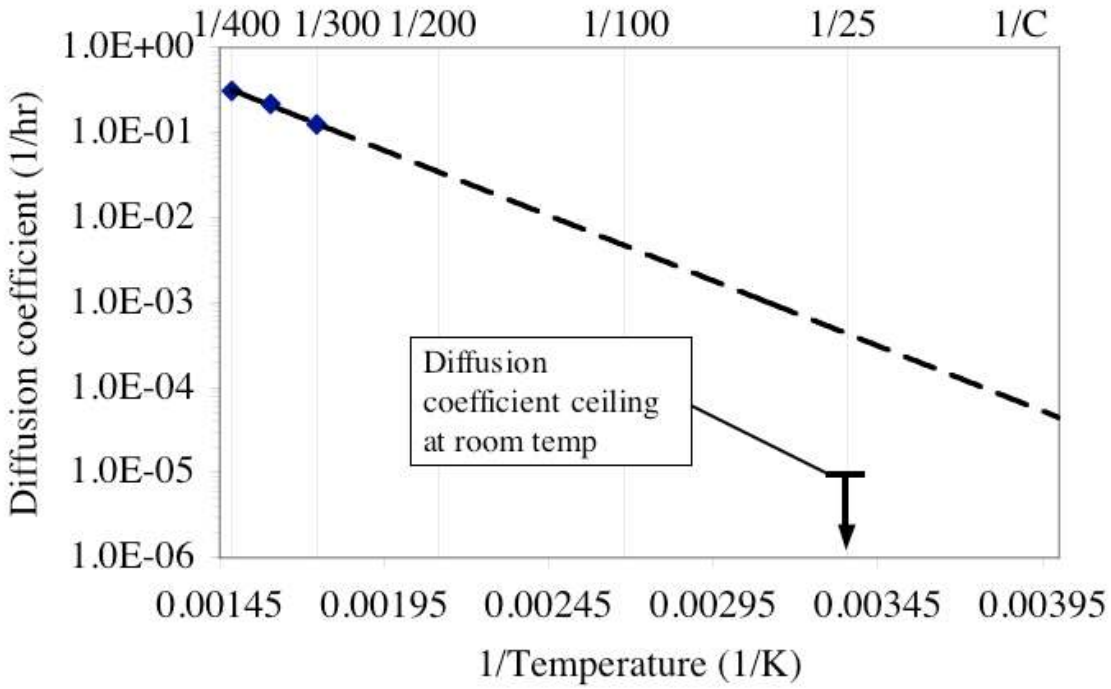

Figure 16. Arrhenius plot of diffusion coefficient and temperature.